

VARIATION IN THE WAVE RESISTANCE  
OF AN AMPHIBIAN AIR-CUSHION VEHICLE  
MOVING OVER A BROKEN-ICE FIELD

V. M. Kozin<sup>1</sup> and A. V. Pogorelova<sup>2</sup>

UDC 532.59:629.576

*The nonstationary rectilinear motion of an amphibian air-cushion vehicle (AACV) on a water surface covered with finely broken ice is considered for various modes of velocity variation. The influence of the water depth, flotation parameters, and mode of motion on the wave resistance of the vehicle is analyzed. Maneuvering methods for increasing or decreasing the wave resistance of AACVs are proposed.*

**Key words:** *an incompressible liquid, finely broken ice, amphibian air-cushion vehicle, nonstationary motion, wave resistance.*

1. This work is a continuation of [1]. The hydrodynamic problem of the motion of an amphibian air-cushion on broken ice (AACV) is modeled by a system of surface pressures [2] which moves above the loaded free surface of a floating liquid [3, 4].

We consider an infinite area covered with broken ice over which the specified system of surface pressures  $q(x, y, t)$  moves at velocity  $u(t)$ . The coordinate system attached to the vehicle is arranged as follows: the  $xOy$  plane coincides with the unperturbed ice–water interface, the  $x$  direction coincides with the direction of motion of the vehicle, and the  $z$  axis is directed vertically upward. It is assumed that water is an ideal incompressible liquid of density  $\rho_2$  and that the motion of the liquid is potential. The surface density of the floating liquid  $m(x, y)$  is given by the continuous function [3]:

$$m(x, y) = \rho_1(x, y)h(x, y) = \rho_1^0 s_1(x, y)h(x, y).$$

Here  $\rho_1(x, y)$  is the ice density “spread” over the liquid surface,  $\rho_1^0$  is the physical density of ice,  $s_1(x, y)$  is a dimensionless function that characterizes the ice density ( $0 \leq s_1 \leq 1$ ), and  $h(x, y)$  is the ice thickness. Below, it is assumed that the quantities  $\rho_1$  and  $h$  are constants.

According to [2, 5], the wave resistance acting on the AACV is calculated by the formula

$$R = \iint_{(\Omega)} q \frac{\partial w}{\partial x} dx dy,$$

where  $\Omega$  is the region of distribution of the load  $q(x, y, t)$  and  $w(x, y, t)$  is the strain of the floating liquid surface, which in linear wave theory is defined in the specified coordinate system as follows [1]:

$$w = -\frac{q}{\rho_2 g} - \frac{1}{g} \frac{\partial \Phi}{\partial t} \Big|_{z=0} + \frac{u}{g} \frac{\partial \Phi}{\partial x} \Big|_{z=0} - \frac{\rho_1 h}{\rho_2 g} \frac{\partial^2 \Phi}{\partial t \partial z} \Big|_{z=0} + \frac{u \rho_1 h}{\rho_2 g} \frac{\partial^2 \Phi}{\partial x \partial z} \Big|_{z=0}.$$

The required velocity potential function  $\Phi(x, y, z, t)$  should satisfy the Laplace equation  $\Delta \Phi = 0$  and the linearized boundary conditions [1]:

---

<sup>1</sup>Komsomol’sk-on-Amur State Technical University, Komsomol’sk-on-Amur 681013. <sup>2</sup>Institute of Materials Science and Metallurgy, Far East Division, Russian Academy of Sciences, Komsomol’sk-on-Amur 681005; sasha@imim.ru. Translated from *Prikladnaya Mekhanika i Tekhnicheskaya Fizika*, Vol. 48, No. 1, pp. 97–102, January–February, 2007. Original article submitted April 14, 2006.

$$\begin{aligned}
& m \left( \frac{\partial^3 \Phi}{\partial t^2 \partial z} - u'_t \frac{\partial^2 \Phi}{\partial x \partial z} - 2u \frac{\partial^3 \Phi}{\partial t \partial x \partial z} + u^2 \frac{\partial^3 \Phi}{\partial x^2 \partial z} \right) \\
& = -\rho_2 g \frac{\partial \Phi}{\partial z} - \rho_2 \left( \frac{\partial^2 \Phi}{\partial t^2} - u'_t \frac{\partial \Phi}{\partial x} - 2u \frac{\partial^2 \Phi}{\partial t \partial x} + u^2 \frac{\partial^2 \Phi}{\partial x^2} \right) - \frac{\partial q}{\partial t} + u \frac{\partial q}{\partial x} \quad \text{for } z = 0, \\
& \frac{\partial \Phi}{\partial z} = 0 \quad \text{for } z = -H
\end{aligned}$$

( $H = H_1 - b$ , where  $H_1$  is the water depth and  $b = \rho_1 h / \rho_2$  is the ice depth under static equilibrium). For great depths where  $H_1$  is much larger than  $h$ , it can be assumed that  $H \approx H_1$ .

Provided that at the time  $t = 0$ , the vehicle does not move and there are no perturbations, except for the static deformation of the free surface, the initial conditions for the function  $\Phi(x, y, z, t)$  are written as [1]

$$\left. \frac{\partial \Phi}{\partial z} \right|_{z=0} = 0, \quad \left. \left( \frac{\partial \Phi}{\partial t} + \frac{\rho_1 h}{\rho_2} \frac{\partial^2 \Phi}{\partial z \partial t} \right) \right|_{t=0} = 0.$$

It is assumed that the vehicle velocity (the system of surface pressures) as a function of time can be approximately expressed by the formula

$$\begin{aligned}
u & = u_1 \tanh(\mu_1 t) + (u_2 - u_1)(\tanh(\mu_2(t - t_2)) + \tanh(\mu_2 t_2))/2 \\
& + (u_3 - u_2)(\tanh(\mu_3(t - t_3)) + \tanh(\mu_3 t_3))/2,
\end{aligned} \tag{1.1}$$

where  $u_1$ ,  $u_2$ , and  $u_3$  are the successive values of the vehicle velocity,  $\mu_1$ ,  $\mu_2$ , and  $\mu_3$  are coefficients that describe the acceleration (deceleration) of the vehicle, the quantities  $t_2$  and  $t_3$  are the times at which the acceleration of the vehicle is equal to  $\mu_2(u_2 - u_1)/2$  and  $\mu_3(u_3 - u_2)/2$ , respectively, and are also points of inflection of the function  $u(t)$ . In the present work, we study various modes of variation of the vehicle velocity (1.1) (modes of motion) as a function of time: 1) acceleration  $\rightarrow$  motion at a specified velocity; 2) deceleration  $\rightarrow$  motion at a specified velocity  $\rightarrow$  deceleration to a complete stop; 3) acceleration  $\rightarrow$  motion at a first specified velocity  $\rightarrow$  acceleration  $\rightarrow$  motion at a second specified velocity; 4) acceleration  $\rightarrow$  motion at a first specified velocity  $\rightarrow$  deceleration  $\rightarrow$  motion at a second specified velocity; 5) acceleration  $\rightarrow$  motion at a specified velocity  $\rightarrow$  deceleration to a complete stop  $\rightarrow$  acceleration  $\rightarrow$  motion at a specified velocity.

According to (1.1), the distance traveled by the vehicle is calculated by the formula

$$\begin{aligned}
s & = \frac{u_1}{\mu_1} \ln(\cosh(\mu_1 t)) + \frac{u_2 - u_1}{2} \left( \frac{1}{\mu_2} \ln \frac{\cosh(\mu_2(t - t_2))}{\cosh(\mu_2 t_2)} + \tanh(\mu_2 t_2) t \right) \\
& + \frac{u_3 - u_2}{2} \left( \frac{1}{\mu_3} \ln \frac{\cosh(\mu_3(t - t_3))}{\cosh(\mu_3 t_3)} + \tanh(\mu_3 t_3) t \right).
\end{aligned} \tag{1.2}$$

As the system of moving pressures  $q(x, y)$  function [1, 6], we use the function

$$q(x, y) = \frac{q_0}{4} \left[ \tanh\left(\alpha_1 \left(x + \frac{L}{2}\right)\right) - \tanh\left(\alpha_1 \left(x - \frac{L}{2}\right)\right) \right] \left[ \tanh\left(\alpha_2 \left(y + \frac{L}{2\omega}\right)\right) - \tanh\left(\alpha_2 \left(y - \frac{L}{2\omega}\right)\right) \right],$$

where  $q_0$  is the nominal pressure,  $L$  is the vehicle length,  $\omega = L/B$  is the vehicle aspect ratio,  $B$  is the vehicle width, and  $\alpha_1$  and  $\alpha_2$  are parameters that characterize the deviation of the pressure distribution in the longitudinal and transverse directions, respectively, from a rectangular shape. The larger the values of  $\alpha_1$  and  $\alpha_2$ , the closer the pressure distribution to a rectangular shape. As  $\alpha_1 \rightarrow \infty$  and  $\alpha_2 \rightarrow \infty$ , the pressure  $q$  is equivalent to the pressure  $q_0$  distributed uniformly over a rectangle. To obtain the best fit between calculation results and experimental data, it is proposed [6] to use the values  $\alpha_1 L = \alpha_2 L = 10$ .

Similarly to [1], the problem is solved analytically using Fourier and Laplace transforms. As a result, we have the following integral formula for the calculation of the wave resistance of the AACV:

$$\frac{R}{D} = \frac{Aq_0}{\rho_2 g L}, \quad D = q_0 L B,$$

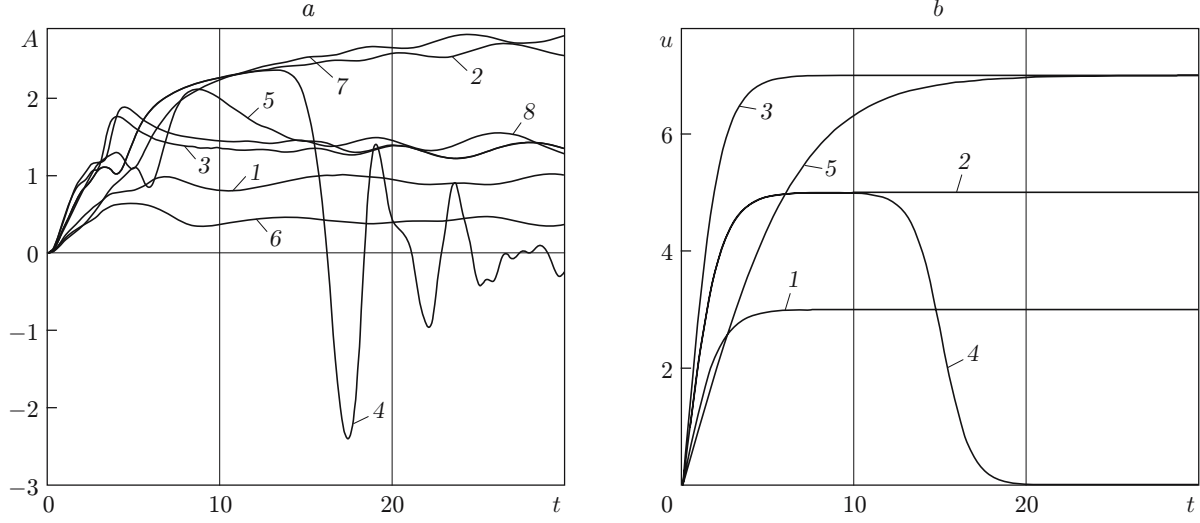


Fig. 1. Wave resistance (a) and velocity of the vehicle (b) versus time for  $H = 3$  m and  $L = 10$  m: 1)  $u_1 = u_2 = u_3 = 3$  m/sec,  $\mu_1 = 0.5 \text{ sec}^{-1}$ , and  $\varepsilon = 0.045$ ; 2)  $u_1 = u_2 = u_3 = 5$  m/sec,  $\mu_1 = 0.5 \text{ c}^{-1}$ , and  $\varepsilon = 0.045$ ; 3)  $u_1 = u_2 = u_3 = 7$  m/sec,  $\mu_1 = 0.5 \text{ sec}^{-1}$ , and  $\varepsilon = 0.045$ ; 4)  $u_1 = 5$  m/sec,  $u_2 = u_3 = 0$ ,  $\mu_1 = 0.5 \text{ sec}^{-1}$ ,  $\mu_2 = 0.6 \text{ sec}^{-1}$ ,  $t_2 = 15$  sec, and  $\varepsilon = 0.045$ ; 5)  $u_1 = u_2 = u_3 = 7$  m/sec,  $\mu_1 = 0.15 \text{ sec}^{-1}$ , and  $\varepsilon = 0.045$ ; 6)  $u_1 = u_2 = u_3 = 3$  m/sec,  $\mu_1 = 0.5 \text{ sec}^{-1}$ , and  $\varepsilon = 0$ ; 7)  $u_1 = u_2 = u_3 = 5$  m/sec,  $\mu_1 = 0.5 \text{ sec}^{-1}$ , and  $\varepsilon = 0$ ; 8)  $u_1 = u_2 = u_3 = 7$  m/sec,  $\mu_1 = 0.5 \text{ sec}^{-1}$ , and  $\varepsilon = 0$ .

$$A = \frac{\pi^2 \omega}{2(\alpha_1 \alpha_2)^2 L} \int_0^t u(\tau) \int_0^\infty \cos\left((t - \tau) \sqrt{\frac{g \rho_2 \lambda \tanh(\lambda H)}{\rho_1 h \lambda \tanh(\lambda H) + \rho_2}}\right) \lambda \times \int_{-\lambda}^{\lambda} \cos(\alpha(s(t) - s(\tau))) \frac{\sin^2(\alpha L/2) \sin^2(\sqrt{\lambda^2 - \alpha^2} L/(2\omega)) \alpha^2}{\sinh^2(\pi \alpha/(2\alpha_1)) \sinh^2(\pi \sqrt{\lambda^2 - \alpha^2}/(2\alpha_2)) \sqrt{\lambda^2 - \alpha^2}} d\alpha d\lambda d\tau. \quad (1.3)$$

Here  $u(\tau)$  is calculated by formula (1.1) and  $s(t)$  and  $s(\tau)$  are calculated by formula (1.2).

2. Numerical calculations using formula (1.3) were performed for  $\alpha_1 L = \alpha_2 L = 10$ ,  $\rho_1^0 = 900 \text{ kg/m}^3$ ,  $\rho_2 = 1000 \text{ kg/m}^3$ , and  $\omega = 2$ .

Figure 1a shows the wave resistance of the vehicle versus time for  $H = 3$  m and  $L = 10$  m [ $\varepsilon = \rho_1 h / (\rho_2 L)$  is the flotation parameter]. Curves 1–5 for broken ice correspond to the modes of velocity variation shown in Fig. 1b for curves with the same numbers. Curves 6–8 in Fig. 1a for pure water correspond to the modes of velocity variation shown in Fig. 1b by curves 1–3. From the results of analysis of Fig. 1b, it follows that the wave resistance of the vehicle depends significantly on the velocity to which it is accelerated. Usually, the velocities at which the vehicle has the maximum wave resistance are called the critical velocities. In Fig. 1a, curves 1 and 6 correspond to the wave resistance of the vehicle at a subcritical velocity in the first mode of motion, curves 2 and 7 correspond to the wave resistance of the vehicle at a near-critical velocity, and curves 3 and 8 to the wave resistance at a supercritical velocity. It is evident that the maximum wave resistance of the vehicle is reached when it moves at the critical velocity. In the case of motion over broken ice, the wave resistance of the vehicle is higher at subcritical velocities and is slightly lower at the critical and supercritical velocities than the wave resistance of the vehicle moving over pure water (in the stationary mode). This conclusion agrees with the results of [7] obtained for the stationary motion of AACVs. In addition, with time, curves 1–3 and 6–8 reach stationary values [6, 7] of the wave resistance, after which they hardly vary, retaining the undulating nature. From an analysis of curve 4 in Fig. 1a, it follows that during deceleration of the vehicle to zero velocity, the wave resistance changes sign several times and tends to zero in an undulating manner. This behavior of the wave resistance may be explained by the fact that during deceleration, the hydrodynamic wave overtakes the vehicle. In this case, the AACV first falls on the wave trough and then appears on the side of the wave where  $\partial w / \partial x < 0$ , after which the vehicle appears on the crest of the next

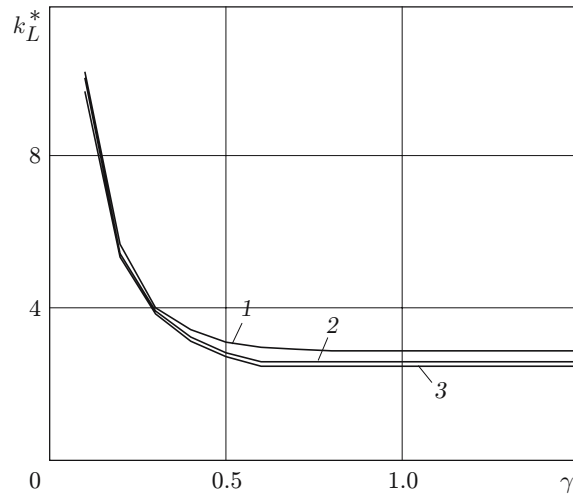


Fig. 2. Dimensionless critical velocity parameter  $k_L^*$  versus dimensionless depth  $\gamma$  for  $\varepsilon = 0.045$  (1), 0.0225, and 0 (3).

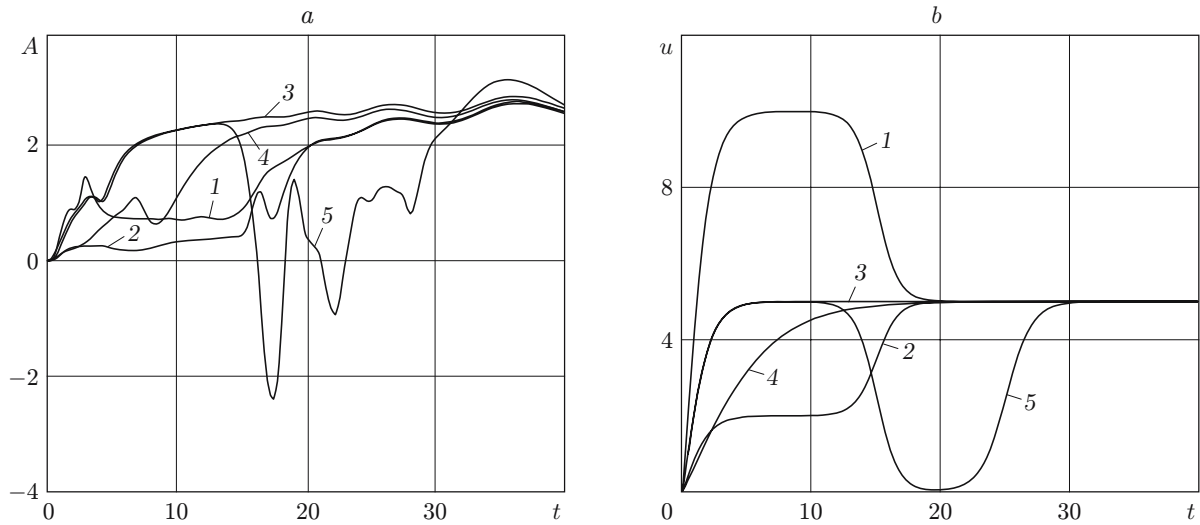


Fig. 3. Wave resistance (a) and velocity (b) of the AACV versus time for various modes of reaching the critical velocity ( $H = 3$  m,  $L = 10$  m,  $\varepsilon = 0.045$ ,  $\mu_2 = 0.6$  sec $^{-1}$ , and  $t_2 = 15$  sec): 1)  $u_1 = 10$  m/sec,  $u_2 = u_3 = 5$  m/sec, and  $\mu_1 = 0.5$  sec $^{-1}$ ; 2)  $u_1 = 2$  m/sec,  $u_2 = u_3 = 5$  m/sec, and  $\mu_1 = 0.5$  sec $^{-1}$ ; 3)  $u_1 = u_2 = u_3 = 5$  m/sec and  $\mu_1 = 0.5$  sec $^{-1}$ ; 4)  $u_1 = u_2 = u_3 = 5$  m/sec and  $\mu_1 = 0.15$  sec $^{-1}$ ; 5)  $u_1 = 5$  m/sec,  $u_2 = 0$ ,  $u_3 = 5$  m/sec,  $\mu_1 = 0.5$  sec $^{-1}$ ,  $\mu_3 = 0.5$  sec $^{-1}$ , and  $t_3 = 25$  sec.

wave which followed it, etc. After all hydrodynamic waves overtake the vehicle, its wave resistance decreases to zero. An analysis of the behavior of curves 3 and 5 in Fig. 1a shows that the higher the initial acceleration (curve 3), the smaller the main hump of the wave resistance when the vehicle reaches the supercritical velocity in the first mode of motion. We note that in the first mode of motion, the initial acceleration is  $a = \mu_1 u_1$ . Thus, to reach the specified supercritical velocity at the lowest wave resistance, the AACV needs to be accelerated to this velocity at the maximum acceleration.

As is known, for the stationary and uniformly accelerated modes of motion of AACVs, the critical velocity depends on the water depth [1, 6, 7]. Figure 2 shows curves of the dimensionless critical velocity parameter  $k_L^* = gL/u_1^2$  for the vehicle moving in the first mode versus the dimensionless water depth parameter  $\gamma = H/L$ . These curves correspond to both the stationary [7] and uniformly accelerated motions of AACVs in broken ice [1] and pure water [6].

Figure 3 shows curves of the wave resistance and velocity of the vehicle versus time for various modes of reaching the critical velocity in the first, third, fourth, and fifth modes of motion for  $H = 3$  m,  $L = 10$  m,  $\varepsilon = \rho_1 h / (\rho_2 L) = 0.045$ ,  $\mu_2 = 0.6 \text{ sec}^{-1}$ , and  $t_2 = 15$  sec. Curves 1 and 2 correspond to the wave resistance when the vehicle reaches the critical velocity in the fourth and third modes of motion. Curves 3 and 4 correspond to the wave resistance when the vehicle reaches the critical velocity in the first mode of motion at initial accelerations  $a = 2.5$  and  $0.75 \text{ m/sec}^2$ , respectively. From an analysis of curves 3 and 4, it follows that the maximum wave resistance is attained more quickly when the vehicle reaches the critical velocity in the first mode of motion at the highest acceleration. When the critical velocity is reached in the third and fourth modes of motion (curves 2 and 1), the wave resistance, though tending to the critical value, does not take the maximum values corresponding to the given critical velocity. Curve 5 in Fig. 3a corresponds to the wave resistance when the vehicle reaches the critical velocity in the fifth mode of motion. In this mode, where the vehicle reaches the critical velocity, then decelerates to a complete stop, and reaches the critical velocity again, higher wave resistances are attained.

**3.** An analysis of the results leads to the following conclusions. For a vehicle moving in broken ice, the maximum wave resistance arises when the vehicle reaches the critical velocity, which depends on the water depth, the vehicle performance, and the flotation parameter. To reduce the wave resistance, it is recommended to move at a subcritical velocity or to reach a specified supercritical velocity at the maximum acceleration. In icebreaking activities intended to break fast ice, to further crush broken ice or to eliminate ice jams and gorges, which can cause catastrophic floods, it is expedient to use the mode of motion of AACVs with the maximum wave steepness. For this, it is recommended that the vehicle be moved in the fifth mode, i.e., it should reach the critical velocity, then decelerate, and after the wave overtakes the vehicle, reach the critical velocity again.

This work was supported by the Program “Development of the Scientific Potential of the Higher School (2006–2008)” (Grant No. RNP.2.1.2.1809).

## REFERENCES

1. V. M. Kozin and A. V. Pogorelova, “Effect of broken ice on the wave resistance of an amphibian air-cushion vehicle in nonstationary motion,” *J. Appl. Mech. Tech. Phys.*, **40**, No. 6, 1036–1041 (1999).
2. Yu. Yu. Benua, V. K. D’yachenko, B. A. Kolyzaev, et al., *Foundations of the Theory of Air-Cushion Vehicles* [in Russian], Sudostroenie, Leningrad (1970).
3. D. E. Kheisin, *Ice Cover Dynamics* [in Russian], Gidrometeoizdat, Leningrad (1967).
4. S. A. Gabov, “One hydrodynamic problem of an ideal liquid related to flotation,” *Diff. Uravn.*, **24**, No. 1, 16–21 (1988).
5. V. P. Bol’shakov, “Wave resistance of a system of surface pressures,” in: *Proc. XIII Scientific Conf. of the Scientific-Research Society of the Ship Building Industry on Ship Theory* (Leningrad, September 10–15, 1963), Issue 49, Krylov Inst., Leningrad (1963), pp. 68–88.
6. L. J. Doctors and S. D. Sharma, “The wave resistance of an air-cushion vehicle in steady and acceleration motion,” *J. Ship Res.*, **16**, No. 4, 248–260 (1972).
7. V. M. Kozin and A. V. Milovanova, “The wave resistance of amphibian air-cushion vehicles in broken ice,” *J. Appl. Mech. Tech. Phys.*, **37**, No. 5 634–637 (1996).